山西大学学报(自然科学版)47(5):1086—1096,2024
Journal of Shanxi University(Nat. Sci. Ed.)

DOI:10.13451/j.sxu.ns.2024110

单宁酸与人血清白蛋白互作的分子动力学分析和实验验证

田鹏[1],宋洁[1],赵成鹏[1],张晨玉[1],武棒棒[2],赵春贵[3]
(1.山西工程科技职业大学 体育学院,山西 太原 030619;
2.山西省农业科学院小麦研究所,山西 临汾 041000;
3.华侨大学 化工学院,福建 泉州 362021)

摘 要:本文通过荧光光谱、酶解和分子对接等技术研究了单宁酸(TA)与人血清白蛋白(HSA)之间的仿生作用力和分子动力学模拟。结果表明,TA与HSA的相互作用是一个典型的两阶段反应:快反应阶段(RRS)和慢反应阶段(SRS)。在25 ℃时,结合常数分别为3.16×10^5 L·mol^{-1}和3.55×10^8 L·mol^{-1}。荧光光谱表明TA对HSA的猝灭机理是静态猝灭效应,且疏水力在TA与HSA相互作用过程中起着重要作用。基于Förster非辐射能量转移理论,确定TA的结合位点位于亚结构域A的疏水区域,TA与人血清白蛋白Trp212之间的距离分别为2.21 nm(RRS)和1.97 nm (SRS)。疏水探针和酶解实验证实TA与HSA之间的相互作用分为两个独立的过程,包括快速反应中的瞬时识别并耦合及慢速反应中的再匹配。本研究验证了TA与HSA的相互作用力,并阐明其反应过程,为植物多酚与蛋白质互作模式的研究提供了参考依据。

关键词:快反应;慢反应;荧光光谱;分子对接
中图分类号:Q946 **文献标志码:**A **文章编号:**0253-2395(2024)05-1086-11

The Molecular Dynamics and Experimental Verification of the Interaction Between Tannic Acid and Human Serum Albumin Protein

TIAN Peng[1], SONG Jie[1], ZHAO Chengpeng[1], ZHANG Chenyu[1], WU Bangbang[2], ZHAO Chungui[3]
(1. *College of Physical Education, Shanxi Vocational University of Engineering Science and Technology, Taiyuan* 030619*, China;*
2. *Institute of Wheat Research, Shanxi Academy of Agricultural Sciences, Linfen* 041000*, China;*
3. *College of Chemical Engineering, Huaqiao University, Quanzhou* 362021*, China*)

Abstract: This study examines the interaction between tannic acid (TA) and human serum albumin (HSA) using fluorescence spectroscopy, enzymolysis and molecular docking techniques. The results reveal that the interaction process between TA and HSA could be regarded as a typical two-stage reaction: a rapid reaction stage (RRS) and a slow reaction stage (SRS). The binding constants at 25 ℃ are determined to be 3.16×10^5 L•mol^{-1} and 3.55×10^8 L•mol^{-1}, respectively. The analysis of the fluorescence spectra indicates that TA quenches HSA through a static quenching mechanism, with hydrophobic forces playing a significant role in the binding process. Based on the Förster non-radiative energy transfer theory, the binding site of TA is identified as the hydrophobic region of subdomain A. The distance between TA and HSA Trp212 are measured to be 2.21 nm in RRS and 1.97 nm in SRS, respectively. Hydrophobic probe and enzymatic hydrolysis analysis, confirmed that the interaction between TA and HSA was divided into two independent processes, including instantaneous recognition and coupling in the fast reaction and rematching in the slow reaction. In conclusion, this study provides clarification on the interaction mechanism and reaction process between TA and HSA, thereby enhancing our understanding of the interaction between plant polyphenols and proteins.

收稿日期:2024-02-08;**接受日期:**2024-06-10
基金项目:山西省教育科学"十四五"规划课题(TY-230016);山西省哲学社会科学项目(2023YJ148)
作者简介:田鹏(1983-),男,山西沁县人,硕士,副教授,研究方向为运动人体科学。E-mail:tianpeng@sxgkd.edu.cn
引文格式:田鹏,宋洁,赵成鹏,等.单宁酸与人血清白蛋白互作的分子动力学分析和实验验证[J].山西大学学报(自然科学版),2024,47(5):1086-1096. DOI:10.13451/j.sxu.ns.2024110

Key words: rapid reaction; slow reaction; fluorescence spectra; molecular docking

0 Introduction

Tannic acid (TA) is a hydrolysable tannin polyphenol compound derived from plants. It forms interactions with proteins and polysaccharides through hydrogen bonding, electrostatic, coordinative bonding, and hydrophobic interactions. TA is widely utilized for its anti-cancer, anti-bacterial, and food antioxidant properties[1-3]. The ability to interact and bind with proteins is considered as the most crucial factor in generating biological effects[4-5]. TA is found in various foods, red wine and tea. However, tannins can also reduce the permeability of the human intestinal wall and affect the digestion[6]. Additionally, the complex formed by tannins and proteins interferes with the absorption and utilization of protein nutrients[7]. TA represents the fundamental functional unit of plant tannins, with its primary structure being glucose oligohydroxyl. Therefore, using tannic acid as a model substance to study its interaction mechanism with proteins is representative and universally applicable. Human serum albumin (HSA) is a monomeric protein comprising 585 amino acids, organized into three α-helical domains (I, II and III) containing two subdomains (A and B) within each α-helical domain[8]. One of the most important biological functions of albumins is their ability to transport endogenous and exogenous substances[9-10]. HSA serves as a model protein which is extensively used to study interactions with small molecules[11-12]. It is also employed as a standard product to eliminate the influence of non-uniform structure.

Various methods have been employed to analyze the tannin-protein complexes, including HPLC[13], UV-Vis[14], turbidimetry, electrophoresis[15], and infrared imaging spectroscopy[16-17]. Several models and theories have been reported and discussed, such as the hydrophobic action and multi-point hydrogen bonding theory[18], the selective rule of tannin-protein mutual recognition, the glove-hand action mode[19], the tannin-protein co-precipitation and precipitation mechanism[20]. In recent years, it has been proposed that the plant polyphenols approach the protein molecule surface through hydrophobic interactions, followed by the occurrence of multi-point hydrogen bonding[21]. The extent of binding is influenced by the structure of polyphenols[22-23]. The rapid binding between polyphenols and peptides leads to the conformational changes in the synthesized peptides[24]. Among these theories, "the hydrophobic action and multi-point hydrogen bonding theory" is the most popular, although research on its reaction process is limited. Therefore, this work aims to supplement a possible mechanism for the reaction process.

It is important to explore the interaction mechanism between TA and biological proteins to enhance nutrient absorption and promote human health. Plant tannins have glucosamine skeletons with hydroxyl groups attached to the periphery of different sugars. The structure of TA is the simplest, and if it undergoes two reaction processes, it is likely that other polyhydroxy tannins also undergo them. In fact, it is the interaction between hydroxyl groups and proteins. In this study, the binding process of TA to HSA was analyzed using fluorescence spectroscopy, docking and molecular dynamics simulation. The relationship between the protein hydrophobic domain and polyphenols was investigated using the hydrophobic probe 2-P-toluidinylnaphthalene-6-sulfonate (TNS) and enzymatic hydrolysis, revealing that this interaction was based on the tertiary structure of protein. A possible mechanism of "conformational rematch" for this interaction is proposed in this work.

1 Materials and Methods

1.1 Apparatus

All fluorescence analysis was conducted using the Hitachi F-4500 spectrofluorometer. The absorp-

tion spectrum was obtained by using the Hitachi UV-2010 spectrophotometer. The pH values were measured by using the Inolab digital pH meter.

1.2 Materials and main reagents

Hepes (N-(2-hydroxyerhyl) piperazine-2-erhanesulfonic acid) was obtained from Kermel Chemical Reagent Co, Ltd. (Tianjin, China), while TA and TNS were acquired from Sigma Co, Ltd. (St. Louis, MO, USA). Additionally, HSA was sourced from Solarbio Co., Ltd. (Beijing, China). All of chemicals used in this study were of analytical grade.

1.3 Docking procedure

The crystal structure of HSA (1N5U) was obtained from the Protein Data Bank (https://www.rcsb.org/pdb). The original crystal structure of HSA was processed using Auto Dock Tools 4.2.6. This involved removing non-polar molecules, adding all hydrogen atoms, and preserving the original charge of OVA before exporting it as a. pdbqt file. The 3D structure of TA was drawn using ChemOffice 18.0, which was further processed with Auto Dock Tools 1.5.6 to Generate a. pdb file for the docking study. The protein-ligand complexes with the lowest energies were selected as experimental models. The docking conformations of these complexes were then examined using PyMol.

1.4 Molecular dynamics simulation

A molecular dynamics simulation was conducted according to the procedure reported by Fani et al[25] with some modifications. A 10 ns molecular dynamics simulation was performed using the Gromacs 2019 software package. The CHARMM36 force field was used, and the topology file and small molecule charge were generated using the website https://cgenff. paramchem. org/. A dodecahedron box was selected and filled with solvent before undergoing energy minimization and optimization. Following the energy minimization process, an isothermal-isobaric ensemble (NPT) simulation was performed. This involved applying a constant pressure of 101.325 kPa at a constant temperature of 300 K for a duration of 100 ps. Finally, a 10 ns molecular dynamics simulation was performed.

1.5 Preparation of samples

A 2 mL solution of human serum albumin (HAS) with a concentration of 5×10^{-6} mol·L^{-1} was subjected to titration by a solution of tartaric acid (TA) at a pH of 7.4 at room temperature. A 10 mL aliquot of HSA solution were mixed with an appropriate amount (0~250 μL) of 1×10^{-6} mol·L^{-1} TA solution in volumetric flask to the final concentration of 5×10^{-6} mol·L^{-1}. Then it was shaken and equilibrated for 24 h at 25 ℃ and 37 ℃, respectively.

For the fluorescence measurements, an excitation wavelength of 295 nm was used with the excitation, and emission slits set at 10 nm each. The fluorescent spectrum was recorded in the range of 300 to 600 nm. All solutions were prepared using 0.01 mol·L^{-1} Hepes buffer solutions (pH 7.4) to maintain the ionic strength, a 0.1 mol·L^{-1} sodium chloride (NaCl) solution was employed. Furthermore, all solutions were prepared using Ultra-pure water obtained from a Milli-Q water purification system and stored at 4 ℃.

1.6 SDS−PAGE analysis

HSA and TA were mixed with ratio of 1 ∶ 0.2 for 1 h, 3 h, 9 h and 16 h, and the compounds were incubated with 0.1 mg·mL^{-1} trypsin at 37 ℃ for 40 min. Then the incubation mixtures were separated by Sodium dodecyl sulfate polyacrylamide gel electrophoresis (SDS-PAGE) with a separating gel composing of 10% acrylamide[26]. Then the gels were stained in the fluorescent gel stain solution, and were washed with sterile deionized water, photographed and analyzed.

1.7 Statistical analysis

Analyses of variance and regression equations were performed using SASv9.

2 Results and Discussion

2.1 Molecular docking and co−acting forces in the HAS−TA complex

It has been reported that, the II A and III A in HSA are the most common binding sites[27-28]. The sta-

bility of a ligand-protein complex is directly correlated with its binding affinity, with lower energy values indicating stronger stability. As depicted in the Fig. 1(b), the conformation with the lowest binding energy (−12.6 kcal·mol^{-1}), which suggested the formation of a stable complex between TA and HSA.

Given the presence of numerous hydroxyl groups in TA, hydrogen bonding plays pivotal role in the interaction between TA and HSA. Seventeen hydrogen bonds were identified in the docking model (Fig. 1(a)), including Tyr148 (2.6 Å), Tyr150 (2.4 Å), Arg160 (2.8 Å), Glu188 (2.8 Å), Lys199 (1.8 Å), Trp214 (2.5 Å), Arg218 (2.3 Å), Gln221 (2.3 Å), Arg222 (2.2 Å), Arg257 (2.6 Å), His242 (2.0 Å), Ala261 (2.5 Å), Glu292 (2.7 Å), Asn295 (2.4 Å), Lys444 (2.6 Å), Asp451 (1.9 Å), and Ser454 (2.3 Å). Additionally, π-π stacking occurred in TA harboring rich benzene rings and HSA containing phenyl amino acids (Tyr452, Phe156, Phe157, Phe149, Tyr150, Phe223, Phe211). In summary, the binding of HSA-TA is facilitated by hydrogen bonding, π-π accumulation and hydrophobic interactions, ultimately leading to structural modifications in HSA.

2. 2 Molecular dynamics simulation

The dynamics analysis of the binding between TA and HAS was conducted using molecular dynamics simulation. The conformational changes of HSA were assessed by calculating parameters such as root mean square deviation (RMSD), root mean square fluctuation (RMSF) and radius of gyration (R_g). The RMSD is a statistical measure that describes conformational deviations, and reflects the stability of the system. On the other hand, RMSF is employed to investigate the flexibility of protein residues by means of residue analysis. As shown in Fig. 2(a), the RMSD value exhibited the fluctuations throughout the whole simulation process of HSA-TA complex, suggesting the formation a stable complex and a tendency towards system stability. However, the RMSF value of amino acid residues 120−130, 180−200 and 290−310 in the HSA-TA system was significantly higher than that in the HSA system, indicating that the binding of HSA-TA had a greater impact on amino acid residues at these sites (Fig. 2 (b)). Additionally, the R_g value was utilized to measure the compactness of the HSA structure. A higher R_g value indicates, a looser structure. As illustrated in Fig. 2(c), the R_g value of the HSA-TA complex, generally exceeded that of the HSA, implying that the interaction between TA and HSA led to the exclusion of amino acid residues, thereby disrupting the spiral and folded structure, and resulting in an expanded system.

2. 3 Influence of reaction time

Previous studies have reported that the interactions between polyphenols such as ellagic acid (EA), epigallocatechin gallate (EGCG), epicatechingallate (ECG) and gallic acid (GA) and HSA involve only one rapid reaction stage (RRS)[9,29]. In this study, we aimed to investigate the stability of the reaction time between TA and HSA, by monitoring the fluorescence spectrum curve over a period of 24 h. As shown in Fig. 3(a), the fluorescence of the HSA-TA

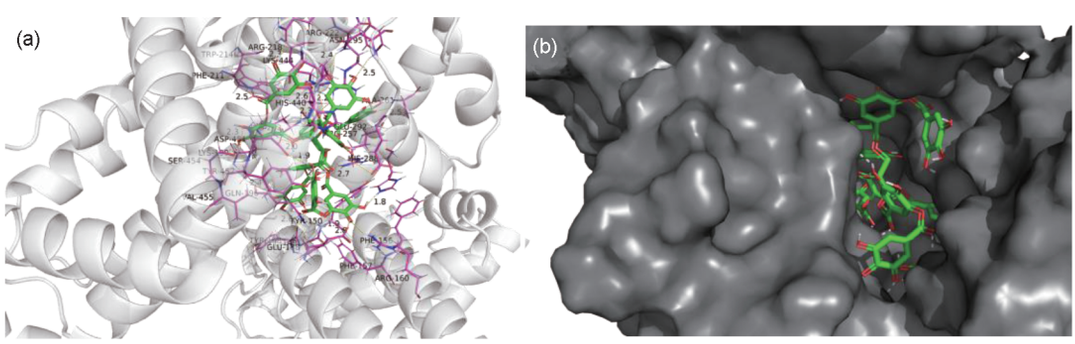

Fig. 1 Molecular docking between HSA and TA

(a) Hydrogen bonding between HSA and TA; (b) The model of interaction between HSA and TA

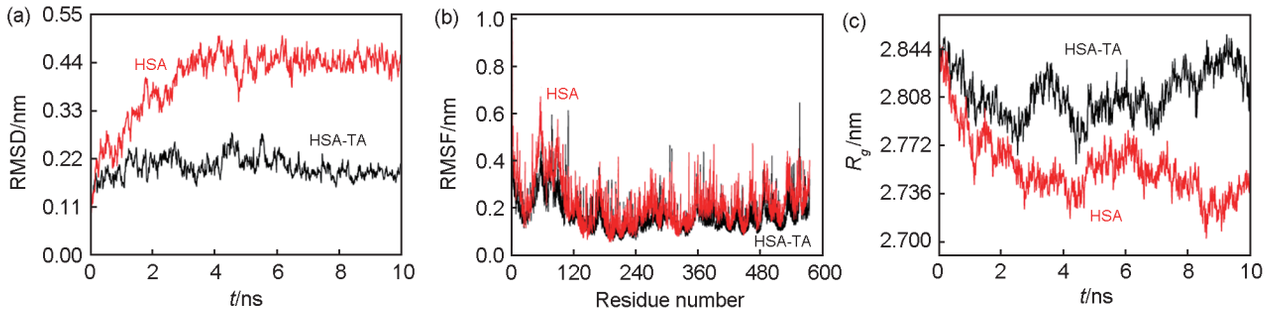

Fig. 2 The molecular dynamics simulations of HSA and HSA-TA

(a and b) RMSD and RMSF of free HSA and HSA-TA complex from 10 ns of molecular dynamics simulations; (c) R_g of free HSA and HSA-TA complex structural superposition of HSA at pecific time from 10 ns molecular dynamics

complex exhibited changes over time, revealing the presence of two distinct reaction stages: the RRS and the slow reaction stage (SRS). Upon addition of TA to the HSA solution, an immediate decrease in fluorescence intensity occurred, followed by a gradual decrease after a stabilization period of 1.5 hours, eventually reaching equilibrium.

2.4 Fluorescence spectrum analysis of HSA−TA

Titration and interaction experiments were conducted to analyze the interaction process between TA and has. It was observed that TA exhibited minimal fluorescence at 345 nm when excited at a wavelength of 295 nm. Therefore, the emission fluorescence detected at 345 nm solely originated from HSA intrinsic contribution unaffected by TA.

As shown in Fig. 3(b), the fluorescence of HSA at 345 nm was quenched by TA gradually, and the similar result was observed at 37 ℃, which indicated that the conformation of HSA might have been changed. Additionally, a red shift in the maximum emission of wavelength of HSA was found upon the addition of TA (Fig. 3(c)). Notably, the impact of TA on HSA fluorescence was observed within a range of specific concentration. Specifically, it was observed that the protein endogenous fluorescence was quenched when the TA concentration was below 4×10^{-6} mol·L^{-1}. Conversely, a significant red shift in the protein's fluorescence spectrum peak occurred when the concentration exceeded 4×10^{-6} mol·L^{-1}. These findings indicate that the binding process of TA resulted in a transition of the tryptophan environment from hydrophobic to hydrophilic, suggesting a significant alteration in protein conformation dependent on TA concentration.

2.5 Quenching mechanism

In general, the differentiation between dynamic and static quenching is based on the regulation of temperature. Therefore, the fluorescence spectra of TA to HSA quenching were examined at the temperature of 25 ℃ and 37 ℃. Subsequently, the Stern-Volmer curves of TA with HSA were constructed. It was observed that the Stern-Volmer plots were exhibited linearity, with the slopes of decreasing as the temperature increased. Furthermore, the results obtained after a 24 h of interaction were consistent with those obtained through titration methods. This preliminary evidence proved the existence of a static quenching interaction between TA and HSA.

To further elucidate the mechanism of fluorescence quenching, the fluorescence quenching data at temperatures of 298 K and 310 K were analyzed using the classical Stern-Volmer equation[30], as depicted in Figure 4(a).

$$\frac{F_0}{F}=1+K_q\tau_0[Q]=1+K_{SV}[Q], \qquad (1)$$

where, F_0 and F are the fluorescence intensity in the absence and presence of quencher (TA), respectively. K_q, K_{sv}, τ_0 and [Q] are the quenching rate constant of the biomolecule, the dynamic quenching constant, the average lifetime of the biomolecule without quencher and the concentration of quencher, respectively. Because the fluorescence lifetime of the biomacromolecule is 10^{-8} s[31], K_{sv} is the slope of the lin-

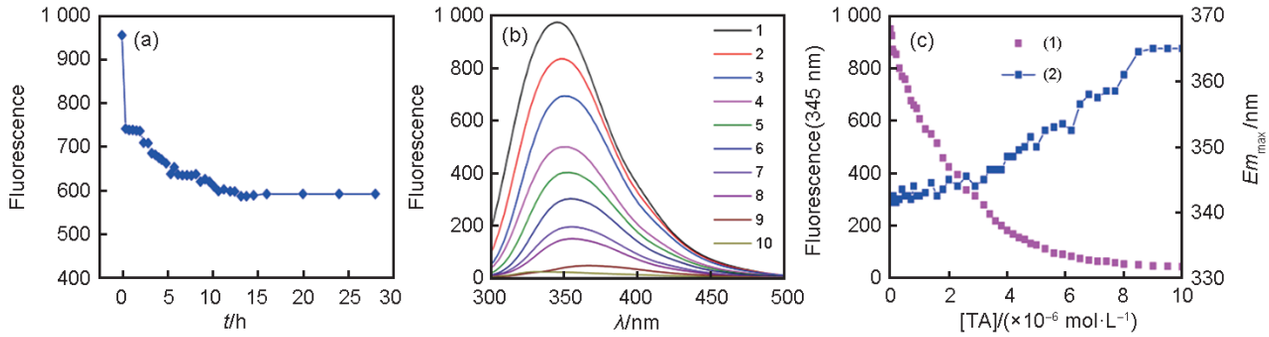

Fig. 3 The fluorescence studies of interactions between HSA and TA

(a) Fluorescence plot. [HSA] =5×10^{-6} mol·L^{-1}, HSA ∶ TA=1 ∶ 0.2. (b) The fluorescence quenching spectrum of 5×10^{-6} mol·L^{-1} HSA (pH=7.4, λ_{ex}=295 nm, T=25 ℃). [TA] / mol·L^{-1} (curve 1—9) : 0; 3.0×10^{-7}; 7.0×10^{-7}; 1.4×10^{-6}; 2.0×10^{-6}; 3.0×10^{-6}; 4.0×10^{-6}; 5.6×10^{-6}; 8.5×10^{-6}. Curve10: the fluorescence of TA. [TA] =5×10^{-6} mol·L^{-1}. (c) The curve of the decreasing fluorescence of HSA at 345 nm. **(1)** The red shift of the maximum emission wavelength of HSA **(2)** the effect of TA on the fluorescence of HSA

ear regression equation (Fig. 4(a)). According to equation (1), the quenching constant K_q can be calculated and is listed in Table 1.

Table 1 The dynamic quenching constants, the quenching rate constant of biomolecule

T/℃	K_{sv}/(L·mol^{-1})	K_q/(L·mol^{-1}·s^{-1})	R^2
25(RRS)	2.98×10^6	2.98×10^{14}	0.994 2
37(RRS)	2.17×10^6	2.17×10^{14}	0.998 2
25(SRS)	6.06×10^5	6.06×10^{13}	0.995 0
37(SRS)	5.52×10^5	5.52×10^{13}	0.991 2

Note: It can be noticed that the magnitude of the quenching constants K_q is in the range of 10^{13}—10^{14}. However, the maximum scatter collision quenching constant of K_q of various quenchers with the biopolymer is 2×10^{10} L·mol^{-1}·s^{-1}[32]. Accordingly, it implies that the quenching is a process of static quenching process, originating from the formation of a complex of HSA and TA.

2.6 Binding constant and binding site analysis

For static quenching, the following equation was employed to calculate the binding constant and the number of binding sites[33]:

$$\lg\frac{F_0-F}{F}=\lg K_A+n\lg[Q], \qquad (2)$$

where, K_A and n are the binding constant and the number of binding sites, respectively. Thus, a plot of $\lg[(F_0-F)/F]$ versus $\lg[Q]$ can be used to determine K_A and n in Fig. 4(b).

The data of K_A and n values were presented in Table 2, indicating the presence or approximately one binding site during the RRS, and nearly two binding sites during the slow reaction stage. However, the temperature demonstrated minimal influence on the binding constant (K_A) of TA and HSA. Notably, the binding constants and binding sites observed during the 24-h interaction (SRS) were higher than those observed during titration (RRS) (Table 2), signifying an increased binding strength between TA and HSA following the slow reaction stage. This suggests that HSA is more readily able to bind additional TA molecules after the initial binding event.

Table 2 The binding constants, the binding sites number of quencher

T/℃	K_A/(L·mol^{-1})	n	R^2
25(RRS)	3.16×10^5	0.86	0.992 8
37(RRS)	9.46×10^5	1.02	0.985 2
25(SRS)	3.55×10^8	1.52	0.991 7
37(SRS)	6.92×10^8	1.58	0.982 5

2.7 Thermodynamic evaluation of the interaction between TA and HSA

The interactions between a drug and a biomolecule are primarily comprised of weak forces, including hydrogen bond formation, van der Waals forces, electrostatic forces, and the hydrophobic interaction. It has been noted that the determination of these interaction forces can be achieved through consideration of the thermodynamic parameters. Specifically, $\triangle H>0$ and $\triangle S>0$ implies hydrophobic interaction; $\triangle H<0$ and $\triangle S<0$ reflects the

van der Waals force or hydrogen bond formation[34]. The thermodynamic parameters can be obtained from the following equations and the results were shown in Table 3:

$$\ln\frac{k_2}{k_1}=\left(\frac{1}{T_1}-\frac{1}{T_2}\right)\frac{\Delta H}{R}, \tag{3}$$

$$\Delta G=-RT\ln K, \tag{4}$$

$$\Delta G=\Delta H-T\Delta S. \tag{5}$$

It can be concluded that the interaction between TA and HSA is thermodynamically spontaneous. The thermodynamic parameters (ΔH and ΔS) as shown in Table 3, are higher than zero, indicating that the predominant forces between TA and HSA are mainly hydrophobic forces. However, it's unavoidable that multi-forces may take part in the interaction at the same time, owing to the intricate structure of HSA and TA, which further complement and validate the results from molecular docking and molecular dynamics simulation analysis.

Table 3 The values of thermodynamic parameters

Mode	$\triangle G$ / (kJ·mol^{-1})	$\triangle H$ / (kJ·mol^{-1})	$\triangle S$ / (J·mol^{-1}·K^{-1})
titration	−24.53	268.83	984
interact 24 h	−36.97	147.39	619

2.8 Transferring energy between TA and HSA

According to Förster non-radiative energy transfer theory[35], HSA functions as a donor and exhibits strong intrinsic fluorescence. The Fig. 4(c) demonstrates the efficient energy transfer that takes place between TA and HSA, due to the considerable spectral overlap between the fluorescence emission spectrum of HSA (2) and the UV absorption spectrum of TA (1).

The energy transfer effect is related not only to the distance between the acceptor and the donor, but also to the critical energy transfer distance. The relation among these factors is:

$$E=\frac{R_0^6}{R_0^6+r^6}, \tag{6}$$

where, r is the distance between the acceptor and the donor, and R_0 is the critical distance when the transfer efficiency is 50%, in turn, which can be calculated by:

$$R_0^6=8.8\times10^{-25}K^2\Phi NJ, \tag{7}$$

where, K^2 is the spatial orientation factor of the dipoles, Φ is the fluorescence quantum yield of the donor, N is the refractive index of the medium, and J is the overlap integral of the fluorescence emission spectrum of the donor and the absorption spectrum of the acceptor. So J can be calculated using the following formula:

$$J=\frac{\sum F_{(\lambda)}\varepsilon_{(\lambda)}\lambda^4\Delta\lambda}{\sum F_{(\lambda)}\Delta\lambda}, \tag{8}$$

where $F_{(\lambda)}$ is the fluorescence intensity of the fluorescent donor at wavelength λ, and $\varepsilon_{(\lambda)}$ is the molar absorptivity at the acceptor wavelength λ. The energy transfer efficiency is given by:

$$E=1-\frac{F}{F_0}, \tag{9}$$

where, J can be evaluated by integrating the spectra in Fig. 4(c) and Eq. (8) for λ= 260-560 nm and can be 1.11×10^{-14} cm^3·L·mol^{-1}. Under these experimental conditions, we found a characteristic distance of R_0 = 2.60 nm, using K^2 = 2/3, N = 1.336, Φ = 0.15[36]. The energy transfer effect E is 0.73 (RRS) and 0.84 (SRS) from Eq. (9) and the maximum distance between TA and tryptophan residue in HSA, Trp212 was 2.21 nm (RRS) and 1.97 nm (SRS). This confirms that the energy transfer between TA and HSA contributes to the decrease of HSA fluorescence intensity. The binding site for TA may be in a hydrophobic region in the sub-domain IIA of HSA. After interaction for 24 h, the distance between TA and tryptophan in HSA decreased, indicating that the combination of TA and HSA was strengthened. It clearly suggested that the slow reaction stage is more stable than the reaction stage.

2.9 Analysis of the binding process using hydrophobic fluorescence probes

TNS is considered as one of most important hydrophobic fluorescent probes in the field of protein research[37]. Upon excitation at a wavelength of 322 nm, the HSA-TNS complex exhibited a strong intensity in fluorescence with the maximum emission at about 440 nm (Fig. 5). This observation indi-

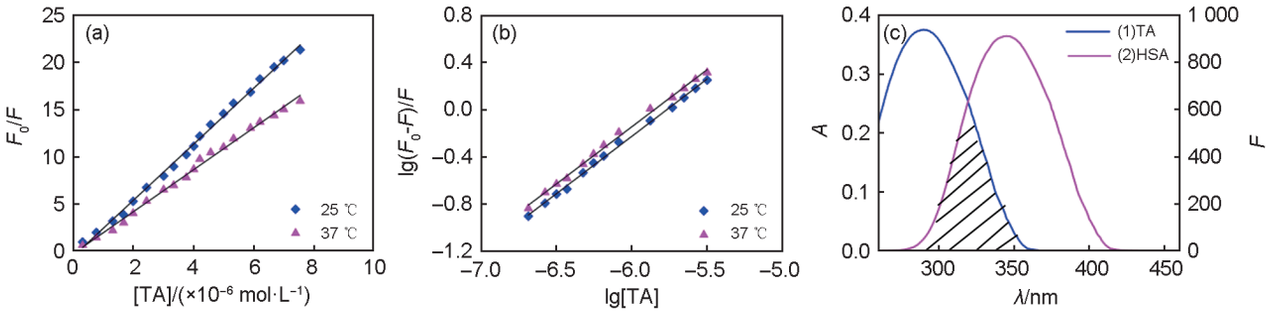

Fig. 4 Fluorescence quenching mechanism of interactions between HSA and TA

(a) Stern-Volmer Plots for the quenching of HSA by TA, λ_{ex}=295 nm, at 25 ℃ and 37 ℃; (b) Plots of lg [(F_0-F)/F] versus lg [TA]. λ_{ex}=295 nm, at different temperatures (25 ℃ and 37 ℃); (c) (**1**) Overlap of the absorption spectra of TA; (**2**) the fluorescence emission spectra of HSA. [HSA]: 5×10^{-6} mol·L^{-1}, [TA]: 5×10^{-6} mol·L^{-1}, in 0.05 mol·L^{-1} Hepes, λ_{ex}=295 nm, T=25 ℃

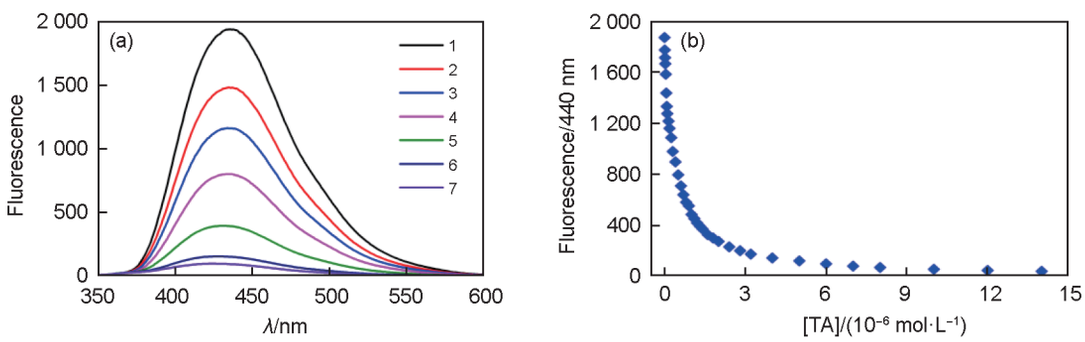

Fig. 5 The binding process between TA and HSA-TNS

(a) The fluorescence quenching spectrum of TA to HSA-TNS at λ_{ex}=322 nm, pH 7.4; [TA] / mol·L^{-1} (curve 1-6): 0, 2.5×10^{-6}, 5×10^{-6}, 1×10^{-5}, 1.5×10^{-5}, 2×10^{-5}; Curve 7 is the fluorescence of HSA without TNS. [HSA] = 5×10^{-6} mol·L^{-1}. (b) The curve of the decreasing fluorescence of HSA-TNS at 440 nm when various concentrations of TA were added

cates that TNS binds to the hydrophobic region of the protein. Furthermore, the addition of TA quenched the fluorescence of HSA-TNS, which affected the hydrophobic environment of TNS.

In addition, the fluorescence was rapidly quenched when the ratio of TA: HSA-TNS was ranged from 0—1, followed by a gradual decline beyond that ratio. This phenomenon indicated that the interaction between TA and HSA does not completed in one step. TA and HSA do not reach the goal in one step, and it has a slow process of rematching, which was consistent with the previous report[38].

2. 10 Interaction analysis of TA and HSA using the enzymolysis method

To further investigate the interaction between HSA and TA, we employed the SDS-PAGE analysis method. The HSA-TA complex formation process was enzymatically treated with trypsin to assess the digestibility of trypsin with respect to the duration of interaction between TA and HSA. As depicted in Fig. 6, after 16 h of interaction between HSA and TA, trypsin basically could not digest the compounds formed by HSA and TA, which suggested that the interaction between TA and HSA was not achieved instantaneously, and the protein complex structure became more stable after the RRS and slow reaction. In a study conducted by Adrian *et al.* In 2022 tannins were found to rapidly bind to short peptides and synthetic peptides resulting in conformational changes in the synthetic polypeptides. So, they concluded that the mechanism of interaction could be TA combined instantaneously with protein[39]. However, after the binding of TA to protein, the conformation of the protein changed gradually to make the binding sites tighter, which could generate a more stable complex. It revealed that rematching of hydrogen bond donors and acceptors, as well

as hydrophobic regions was occurring between TA and the protein, and it was a relatively slow process.

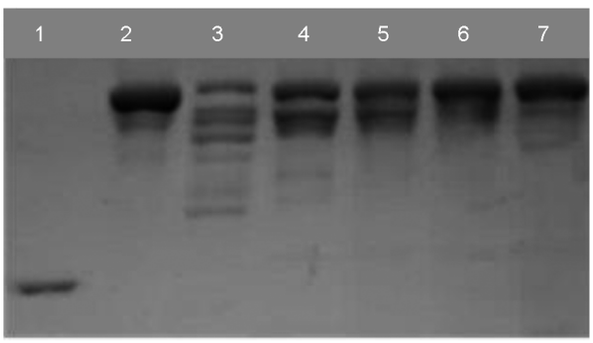

Note: 1: 0.5 mg·mL^{-1} trypsin (MW: 24, 300); 2: 1 mg·mL^{-1} HSA; 3: 0.1 mg·mL^{-1} trypsin and 1 mg·mL^{-1} HSA; 4: HSA interacted with TA for 1 h; 5: HSA interacted with TA for 3 h; 6: HSA interacted with TA for 9 h; 7: HSA interacted with TA for 16 h.

Fig. 6 SDS-PAGE analysis of compounds of HSA and TA digested by trypsin

3 Conclusion

In this study, we investigated the nanoscale bio-inspired interaction analysis of TA and HSA using fluorescence spectroscopy, molecular docking and dynamic modeling. Our findings highlight the significant role of hydrogen bonding during the interaction process between TA and HSA. We observed that the binding ability is similar to that of casein, which containing about 16% proline, although HSA contains about 4% proline. Furthermore, we observed an enhancement in binding ability with an increase in the molecular weight of polyphenol. In addition, our results suggest that the selectivity of TA towards proteins is influenced by variables such as the molecular weight of proteins, proline content, protein structure and pI value. It is worth noting that while the emphasis has traditionally been on the composition of amino acids in the primary structure of proteins, our study underscores the importance of hydrophobic structures formed in the secondary and higher structure of the protein. The results indicate that hydrophobic interactions play a pivotal role in this type of interaction, accompanied by the synergistic effects in the formation of hydrogen bonds. Based on the kinetic model of plant polyphenols-protein reaction, we propose a two-step process: first, a rapid combination through hydrophobic action and hydrogen bonding, second, followed by further conformational changes and rematching, resulting in the fluorescence quenching of the protein. Notably, this study presents, for the first time the "conformational mismatch" hypothesis of the interaction between TA and HSA, providing valuable insights into the interaction between polyphenolic compounds and protein biomolecules.

References:

[1] NIE X H, ZHAO L M, WANG N N, *et al*. Phenolics-protein Interaction Involved in Silver Carp Myofibrilliar Protein Films with Hydrolysable and Condensed Tannins [J]. *LWT Food Sci Technol*, 2017, **81**: 258−264. DOI: 10.1016/j.lwt.2017.04.011.

[2] JAFARI H, GHAFFARI-BOHLOULI P, NIKNEZHAD S V, *et al*. Tannic Acid: a Versatile Polyphenol for Design of Biomedical Hydrogels[J]. *J Mater Chem B*, 2022, **10** (31): 5873−5912. DOI: 10.1039/D2TB01056A.

[3] DENG L, QI Y F, LIU Z H, *et al*. Effect of Tannic Acid on Blood Components and Functions[J]. *Colloids Surf B Biointerfaces*, 2019, **184**: 110505. DOI: 10.1016/j. colsurfb.2019.110505.

[4] YUAN S J, ZHANG Y Y, LIU J X, *et al*. Structure-affinity Relationship of the Binding of Phenolic Acids and Their Derivatives to Bovine Serum Albumin[J]. *Food Chem*, 2019, **278**: 77−83. DOI: 10.1016/j. foodchem.2018.11.060.

[5] STADMILLER S S, AGUILAR J S, PARNHAM S, *et al*. Protein-peptide Binding Energetics under Crowded Conditions[J]. *J Phys Chem B*, 2020, **124**(42): 9297−9309. DOI: 10.1021/acs.jpcb.0c05578.

[6] LI R Y, ZENG Z C, FU G M, *et al*. Formation and Characterization of Tannic Acid/Beta-glucan Complexes: Influence of pH, Ionic Strength, and Temperature[J]. *Food Res Int*, 2019, **120**: 748−755. DOI: 10.1016/j.foodres.2018.11.034.

[7] CHEN Y, HU J, YI X Z, *et al*. Interactions and Emulsifying Properties of Ovalbumin with Tannic Acid[J]. *LWT*, 2018, **95**: 282−288. DOI: 10.1016/j.lwt.2018.04.088.

[8] CZUB M P, VENKATARAMANY B S, MAJOREK K A, *et al*. Testosterone Meets Albumin - the Molecular Mechanism of Sex Hormone Transport by Serum Albumins[J]. *Chem Sci*, 2018, **10**(6): 1607−1618. DOI: 10.1039/c8sc04397c.

[9] HANDING K B, SHABALIN I G, KASSAAR O, *et al*. Circulatory Zinc Transport is Controlled by Distinct Interdomain Sites on Mammalian Albumins[J]. *Chem Sci*, 2016, **7**(11): 6635−6648. DOI: 10.1039/c6sc02267g.

[10] STAII C. Conformational Changes in Surface-immobilized Proteins Measured Using Combined Atomic Force and Fluorescence Microscopy[J]. *Molecules*, 2023, **28**(12): 4632. DOI: 10.3390/molecules28124632.

[11] ZARGAR S, WANI T, ALSAIF N, *et al*. A Comprehensive Investigation of Interactions Between Antipsychotic Drug Quetiapine and Human Serum Albumin Using Multi-spectroscopic, Biochemical, and Molecular Modeling Approaches[J]. *Molecules*, 2022, **27**(8): 2589. DOI: 10.3390/molecules27082589.

[12] SPEDALIERI C, PLAICKNER J, SPEISER E, *et al*. Ultraviolet Resonance Raman Spectra of Serum Albumins[J]. *Appl Spectrosc*, 2023, **77**(9): 1044−1052. DOI: 10.1177/00037028231183728.

[13] SUOMINEN E, SAVILA S, SILLANPÄÄ M, *et al*. Affinity of Tannins to Cellulose: A Chromatographic Tool for Revealing Structure-activity Patterns[J]. *Molecules*, 2023, **28**(14): 5370. DOI: 10.3390/molecules28145370.

[14] ISHTIKHAR M, AHMAD E, SIDDIQUI Z, *et al*. Biophysical Insight into the Interaction Mechanism of Plant Derived Polyphenolic Compound Tannic Acid with Homologous Mammalian Serum Albumins[J]. *Int J Biol Macromol*, 2018, **107**(Pt B): 2450−2464. DOI: 10.1016/j.ijbiomac.2017.10.136.

[15] FILATOVA L, EMELIANOV G, BALABUSHEVICH N, *et al*. Supramolecular Assemblies of Mucin and Lysozyme: Formation and Physicochemical Characterization[J]. *Process Biochem*, 2022, **113**: 97−106. DOI: 10.1016/j.procbio.2021.12.022.

[16] JIA J J, GAO X, HAO M H, *et al*. Comparison of Binding Interaction Between B-lactoglobulin and Three Common Polyphenols Using Multi-spectroscopy and Modeling Methods[J]. *Food Chem*, 2017, **228**: 143−151. DOI: 10.1016/j.foodchem.2017.01.131.

[17] BOU-ABDALLAH F, SPRAGUE S E, SMITH B M, *et al*. Binding Thermodynamics of Diclofenac and Naproxen with Human and Bovine Serum Albumins: a Calorimetric and Spectroscopic Study[J]. *J Chem Thermodyn*, 2016, **103**: 299−309. DOI: 10.1016/j.jct.2016.08.020.

[18] SHTEINIKOV V Y, BARYGIN O I, GMIRO V E, *et al*. Multiple Modes of Action of Hydrophobic Amines and Their Guanidine Analogues on ASIC1a[J]. *Eur J Pharmacol*, 2019, **844**: 183−194. DOI: 10.1016/j.ejphar.2018.12.024.

[19] BARTOCCI A, PEREIRA G, CECCHINI M, *et al*. Capturing the Recognition Dynamics of *para*-sulfonatocalix[4]Arenes by Cytochrome C: Toward a Quantitative Free Energy Assessment[J]. *J Chem Inf Model*, 2022, **62**(24): 6739−6748. DOI: 10.1021/acs.jcim.2c00483.

[20] SIMAS R G, TAKAGI M, MIRANDA E A. Study of the Polyribosyl-ribitol-phosphate Precipitation Mechanism by Salts and Organic Solvents[J]. *Int J Biol Macromol*, 2019, **140**: 102−108. DOI: 10.1016/j.ijbiomac.2019.08.110.

[21] RABBANI G, AHN S N. Structure, Enzymatic Activities, Glycation and Therapeutic Potential of Human Serum Albumin: A Natural Cargo[J]. *Int J Biol Macromol*, 2019, **123**: 979−990. DOI: 10.1016/j.ijbiomac.2018.11.053.

[22] AL-SHABIB N A, KHAN J M, MALIK A, *et al*. Molecular Insight into Binding Behavior of Polyphenol (Rutin) with Beta Lactoglobulin: Spectroscopic, Molecular Docking and MD Simulation Studies[J]. *J Mol Liq*, 2018, **269**: 511−520. DOI: 10.1016/j.molliq.2018.07.122.

[23] GUO N H, WANG C L, SHANG C, *et al*. Integrated Study of the Mechanism of Tyrosinase Inhibition by Baicalein Using Kinetic, Multispectroscopic and Computational Simulation Analyses[J]. *Int J Biol Macromol*, 2018, **118**(Pt A): 57−68. DOI: 10.1016/j.ijbiomac.2018.06.055.

[24] KASPCHAK E, MAFRA L I, MAFRA M R. Effect of Heating and Ionic Strength on the Interaction of Bovine Serum Albumin and the Antinutrients Tannic and Phytic Acids, and Its Influence on in Vitro Protein Digestibility [J]. *Food Chem*, 2018, **252**: 1−8. DOI: 10.1016/j.foodchem.2018.01.089.

[25] FANI N, BORDBAR A K, GHAYEB Y. A Combined Spectroscopic, Docking and Molecular Dynamics Simulation Approach to Probing Binding of a Schiff Base Complex to Human Serum Albumin[J]. *Spectrochim Acta A Mol Biomol Spectrosc*, 2013, **103**: 11−17. DOI: 10.1016/j.saa.2012.11.003.

[26] ZHENG X W, TANG C G, HAN R, *et al*. Identification, Characterization, and Evaluation of Novel Stripe Rust-resistant Wheat-*Thinopyrum intermedium* Chromosome Translocation Lines[J]. *Plant Dis*, 2020, **104**(3): 875−881. DOI: 10.1094/PDIS-01-19-0001-RE.

[27] FANI N, BORDBAR A K, GHAYEB Y. Spectroscopic, Docking and Molecular Dynamics Simulation Studies on the Interaction of Two Schiff Base Complexes with Human Serum Albumin[J]. *J Lumin*, 2013, **141**: 166−172. DOI: 10.1016/j.jlumin.2013.03.001.

[28] RYAN A J, GHUMAN J, ZUNSZAIN P A, *et al*. Structural Basis of Binding of Fluorescent, Site-specific Dan-

sylated Amino Acids to Human Serum Albumin[J]. *J Struct Biol*, 2011, **174**(1): 84−91. DOI: 10.1016/j.jsb.2010.10.004.

[29] KASPCHAK E, GOEDERT A C, IGARASHI-MAFRA L, *et al*. Effect of Divalent Cations on Bovine Serum Albumin (BSA) and Tannic Acid Interaction and Its Influence on Turbidity and in Vitro Protein Digestibility[J]. *Int J Biol Macromol*, 2019, **136**: 486−492. DOI: 10.1016/j.ijbiomac.2019.06.102.

[30] KUIJPERS K P L, BOTTECCHIA C, CAMBIÉ D, *et al*. A Fully Automated Continuous-flow Platform for Fluorescence Quenching Studies and Stern-volmer Analysis[J]. *Angew Chem Int Ed Engl*, 2018, **57**(35): 11278−11282. DOI: 10.1002/anie.201805632.

[31] OSAD'KO I S. Determination of the Efficiency and Energy Transfer Rate in the Fluorescence of a Single Donor-Acceptor Pair Attached to a Biomolecule[J]. *Jetp Lett*, 2018, **107**(11): 725−727. DOI: 10.1134/s0021364018110127.

[32] BHAVYA P, MELAVANKI R, KUSANUR R, *et al*. Effect of Viscosity and Dielectric Constant Variation on Fractional Fluorescence Quenching Analysis of Coumarin Dye in Binary Solvent Mixtures[J]. *Luminescence*, 2018, **33**(5): 933−940. DOI: 10.1002/bio.3492.

[33] İNCI D, AYDıN R, VATAN Ö, *et al*. New Binary Copper(II) Complexes Containing Intercalating Ligands: DNA Interactions, an Unusual Static Quenching Mechanism of BSA and Cytotoxic Activities[J]. *J Biomol Struct Dyn*, 2018, **36**(15): 3878−3901. DOI: 10.1080/07391102.2017.1404936.

[34] VASHEGHANI F B, RAJABI F H, AHMADI M H, *et al*. Stability Constants and Thermodynamic Parameters of some Intermacromolecular Complexes in Relation to Their Specific Interaction Forces[J]. *Polym Bull*, 2005, **55**(6): 437−445. DOI: 10.1007/s00289-005-0447-5.

[35] TOA Z S D, DEGOLIAN M H, JUMPER C C, *et al*. Consistent Model of Ultrafast Energy Transfer in Peridinin Chlorophyll- *a* Protein Using Two-dimensional Electronic Spectroscopy and Förster Theory[J]. *J Phys Chem B*, 2019, **123**(30): 6410−6420. DOI: 10.1021/acs.jpcb.9b04324.

[36] HUANG X W, PENG Y, HUANG J H. Universal Behaviors of Polymer Conformations in Crowded Environment[J]. *Colloid Polym Sci*, 2018, **296**(4): 689−696. DOI: 10.1007/s00396-018-4285-z.

[37] QIU T, KATHAYAT R S, CAO Y, *et al*. A Fluorescent Probe with Improved Water Solubility Permits the Analysis of Protein S-depalmitoylation Activity in Live Cells[J]. *Biochemistry*, 2018, **57**(2): 221−225. DOI: 10.1021/acs.biochem.7b00835.

[38] PANG Y H, YANG L L, SHUANG S M, *et al*. Interaction of Human Serum Albumin with Bendroflumethiazide Studied by Fluorescence Spectroscopy[J]. *J Photochem Photobiol B*, 2005, **80**(2): 139−144. DOI: 10.1016/j.jphotobiol.2005.03.006.

[39] VAKHRUSHEVA T V, SOKOLOV A V, MOROZ G D, *et al*. Effects of Synthetic Short Cationic Antimicrobial Peptides on the Catalytic Activity of Myeloperoxidase, Reducing Its Oxidative Capacity[J]. *Antioxidants*, 2022, **11**(12): 2419. DOI: 10.3390/antiox11122419.